APPLICATION OF THE INFINITE ELEMENT METHOD TO MODELLING THE SURROUNDINGS IN LOW CONTRAST CASES

Artur Poliński *, Jerzy Wtorek** and Bart Truyen***

* Department of Differential Equations, Gdańsk University of Technology, Narutowicza 11/12, 80-952 Gdańsk, Poland
** Department of Biomedical Engineering, Gdańsk University of Technology, Narutowicza 11/12, 80-952 Gdańsk, Poland
*** Department of Electronics and Information Processing, Vrije Universiteit Brussel, Pleinlaan 2, 1050 Brussels, Belgium

apoli@mif.pg.gda.pl

Abstract: The paper presents a comparison between the finite element method (FEM) and infinite FEM, its extension to infinite domains. Three different models are described to demonstrate the differences between FEM and IFEM. Finally, the example is introduced of the application of IFEM to the modelling of a cell for measuring the dielectric parameters of teeth.

Introduction

The modelling of dielectric measurements allows us to understand what we can measure, and to some extent, what measurement error we can expect. The finite element method (FEM) gives very good results for bounded domains. In the case of unbounded domains the FEM models are acceptable if the surroundings are characterised by much lower conductivity and permittivity. In other cases the results obtained from models will be misleading. The alternative in such cases is an extension of the FEM to infinite domains, infinite FEM (IFEM).

The background to IFEM can be found in [1] and [2]. There are different types of infinite elements. An example of the application of two types of these can be found in [3]. We have concentrated on infinite elements with an exponential decay function as they are easy to implement and give good results. The main problem in this lies in making a proper choice of parameter to determine the severity of the decay. A suggestion for calculating its value can be found in [1].

The IFEM has already been tested in some applications of electrical impedance tomography [3], where the problem of truncation of the model near the electrodes was considered, and in modelling the potential distribution for electrical impedance spectroscopy [4], where the current density analysis was used to predict measurement error where the contrast between the measurement material and its surroundings is low.

The paper presents a comparison of the results obtained from FEM and IFEM in certain problems.

Material and Methods

We considered three models in order to show the differences between FEM and IFEM. Finally, the example is presented of the application of IFEM to model a cell for tooth measurement. All the models were constructed in cylindrical co-ordinates with the assumption that the boundary conditions and model properties do not depend on angle. The 3D problem was therefore reduced to a 2D one. Triangular elements were used in all cases. Linear potential approximation was used in each triangular FEM element. The exponential decay function $\exp((r_i-r+z_i-z)/L)$, where (r_i, z_i) are the node co-ordinates and L is a parameter, was considered for all cases in IFEM [1]. The potential distribution was described by the equation

$$\nabla(\sigma^*\nabla u) = 0 \qquad (1)$$

where σ^* is a complex dielectric conductivity ($\sigma^*=\sigma+i\omega\varepsilon$, with σ - conductivity, ε - permittivity, $i=\sqrt{-1}$, and ω - angular frequency) and u is potential. We assume also that the potential equals 0 at infinity, while others boundary conditions depend on the model under consideration.

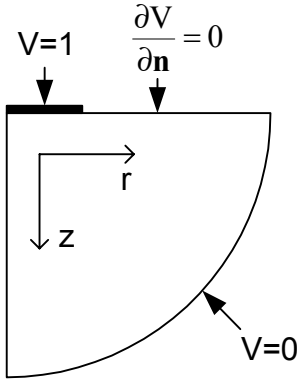

Figure 1: Diagrammatic representation of the single electrode model.

ISSN: 1727-1983

The first model was a single circular electrode in half space (Fig. 1). Five sizes of the first model were considered. The smallest had 400 elements (231 nodes), while the largest had 3,600 elements (1,891 nodes). The electrode had a radius *R*, so the smallest version of the first model was a quarter circle of the radius 2*R*, the following had a radius 3*R*, and so on up to 6*R* for the fifth version of the first model. The conductivity and permittivity multiplied by the angular frequency was equal to 1. In the IFEM model the last layer was constructed using infinite elements.

The second model was a cylinder with a surround (Fig. 2). One of the bases of the cylinder was grounded, while the second was set to the potential 1 V. Again five versions of the model were constructed with different surrounds, so the model ranged in size from 1,600 elements (861 nodes) up to 14,400 elements (7,381 nodes). The radius of the cylinder was equal to *R*, its height to 2*R* and the surround was from *R* to 5*R* in size. The ratio of dielectric properties of the cylinder and its surround varied. The conductivity and permittivity, multiplied by the angular frequency, of the cylinder and surround was set to 1. Next the parameters of the surrounding were changed to 0.1, 1 and 10 respectively, although these changes were not made simultaneously. Again, in the IFEM model, the last layer was constructed using infinite elements.

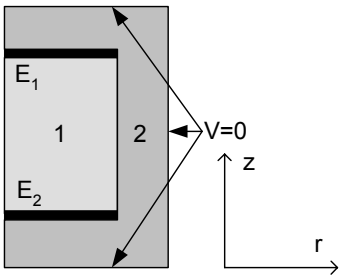

Figure 2: Diagrammatic representation of the cylinder with the surround. Electrodes are marked with bold lines.

The third model was similar to the second (Fig. 3). However, the surround was divided into two parts with different dielectric parameters. The radius of the inner region (marked "1") was equal to 2*R*, the distance between the electrodes 2*R* and the width of the second and third layers (marked "2" and "3") was equal to *R*/2 for the larger version of the model. The outer layer of the smaller version had a width equal to *R*/10. Two different sizes of model were considered. To investigate the influence of linear potential approximation inside the element, a larger variant of the model was created with a dense and coarse mesh, the size of this model being 1,024 elements (561 nodes), 1,600 elements (861 nodes), and 40,000 elements (20,301 nodes). A different distribution of the dielectric parameters inside the models was considered. The inner material (marked "1") has a 10 times greater conductivity and permittivity than the second layer (marked "2"), while the conductivity and permittivity of the outer layer ("3") changed independently from 0.001 up to 0.1 of the value of the middle layer. The potential of one electrode was equal to –1, while the second was +1, (0 on the boundary). The last layer was constructed using infinite elements for the IFEM version of the model.

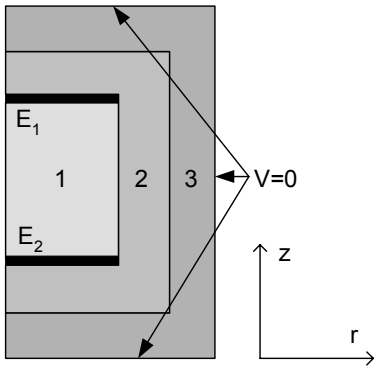

Figure 3: Diagrammatic representation of the third model considered. Electrodes are marked with bold lines and regions of different dielectric parameters by "1", "2" and "3".

The last model is an example of the practical application of IFEM. We have used this method to calculate current density distribution in the model of a cell for the measurement of the dielectric parameters of teeth (Fig. 4). In view of the similarity of these parameters to those of the construction material of the measurement cell and the similarity of the parameters of the construction material to those of air, it is extremely important to know what exactly we are to measure. Conductivity distribution inside the model is explained in Figure 4. The last layer was constructed using infinite elements for the IFEM version of the model.

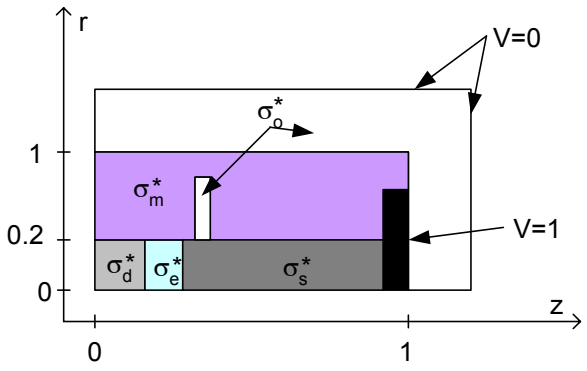

Figure 4: Diagrammatic representation of a cell for measuring the dielectric parameters of teeth (only half is shown). σ^*_m - complex conductivity of the construction material, σ^*_d - complex conductivity of dentine, σ^*_e - complex conductivity of enamel, σ^*_o - complex conductivity of air, σ^*_s - complex conductivity of physiological saline (NaCl).

ISSN: 1727-1983

The base model of the cell consisted of 37,200 elements (18,894 nodes). Three methods of simulation of the surround extending to infinity were considered. In all versions of this model 25 layers of the surround, simulating air, were put in place. In the first method two additional layers near the boundary had diminished complex conductivity (1/10 and 1/100 of the surround respectively, and 1/100 and 1/1,000 respectively in the second version of this model). The second method was based on infinite elements. The third version of the model was on the base of FEM, but with an increased number of elements simulating the surroundings. In each successive third version of the model 10 outer layers of elements were added, so that the 5th model had a size of 85,800 elements (43,344 nodes). These elements had the same conductivity as the surroundings.

In all four IFEM models different values of parameter L were examined (L=5, 10, 100 and 1,000). Smaller values of this parameter caused overflow error in some cases.

Results

The first model shows that the FEM and IFEM give similar results in the range of parameters considered. We observed a difference outside the electrode (Fig. 5), which was dependant on the size of the model and was not larger than 0.032V. The difference between different values of parameter L also can be observed, especially for larger models (Fig. 6 (L=10) and Fig. 7 (L=1,000)).

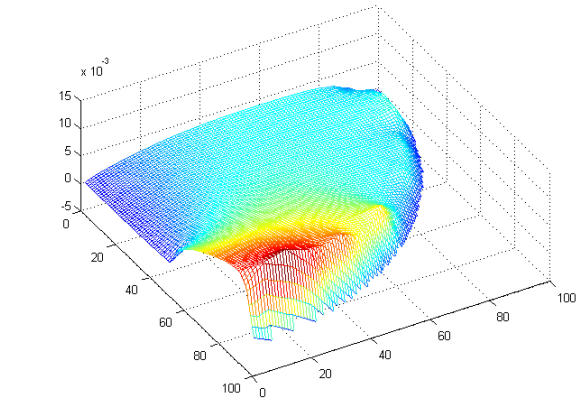

Figure 5: Difference in potential distribution between FEM and IFEM (L=5) for the smallest version of the first model.

The second model enables the non-linear dependence of the results on parameter L to be shown. Figures 8, 9 and 10 show differences in potential distribution between FEM and IFEM for L=5 (Fig. 8), L=10 (Fig. 9), and L=100 (Fig. 10).

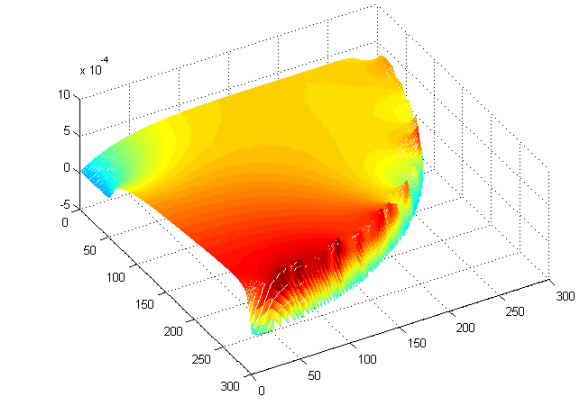

Figure 6: Difference in potential distribution between FEM and IFEM (L=10) for the largest version of the first model.

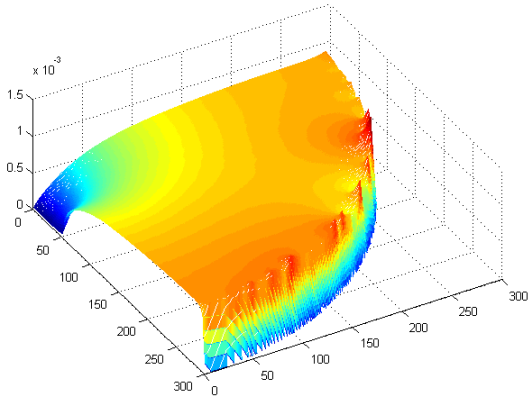

Figure 7: Difference in potential distribution between FEM and IFEM (L=1000) for the largest version of the first model.

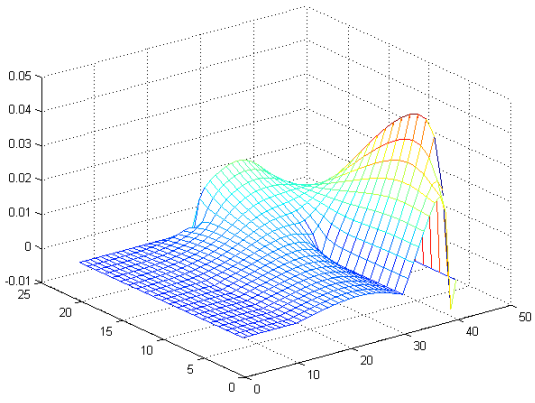

Figure 8: Difference in potential distribution between FEM and IFEM (L=5) for the smallest version of the second model.

ISSN: 1727-1983

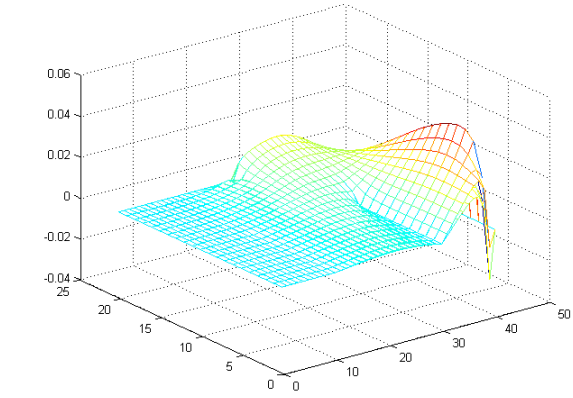

Figure 9: Difference in potential distribution between FEM and IFEM (L=10) for the smallest version of the second model.

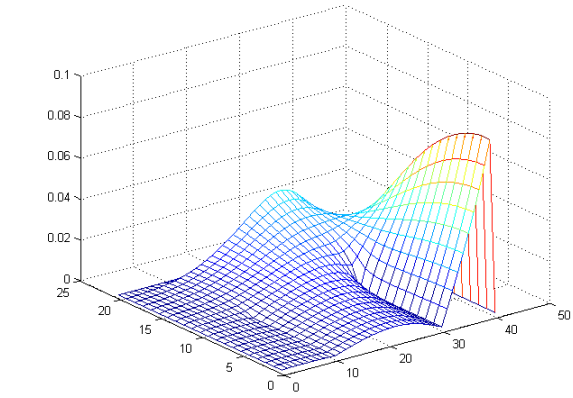

Figure 10: Difference in potential distribution between FEM and IFEM (L=1,000) for the smallest version of the second model.

The maximum difference obtained in potential distribution between FEM and IFEM is greatest for the smallest version of the model, although not greater than 0.1 V (for the larger version of the model it is less than 5e-4 V). In this model the differences in potential distribution between FEM and IFEM can be observed not only in the surround, but also between the electrodes, where they are approximately ten times smaller than the maximum difference outside the cylinder. As regards changes in the conductivity or permittivity of the surround, we also observed a change in phase between potential calculated using FEM and using IFEM (Figs. 11 and 12). Different values of L also cause a different phase shift.

We observed only a very small difference between the results obtained for the ratios of conductivity and permittivity, 1:10 and 1:0.1. The influence of conductivity change observed was very similar to the influence of permittivity change (Figs. 13 and 14).

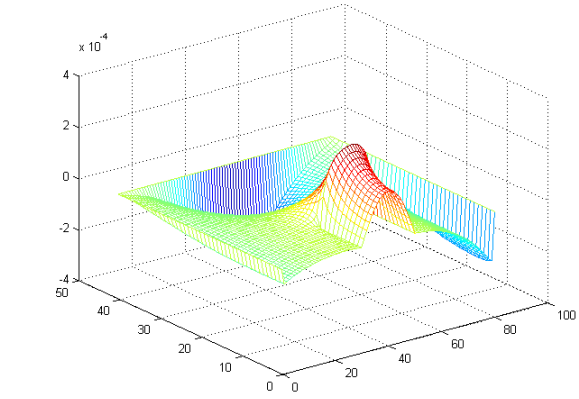

Figure 11: Difference in the real part of the potential distribution between FEM and IFEM (L=100) for the second model.

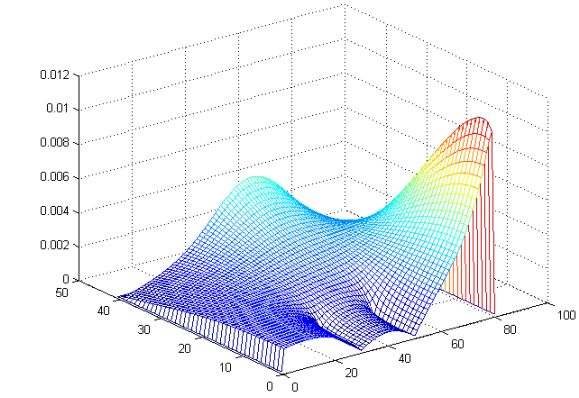

Figure 12: Difference in the imaginary part of the potential distribution between FEM and IFEM (L=100) for the second model.

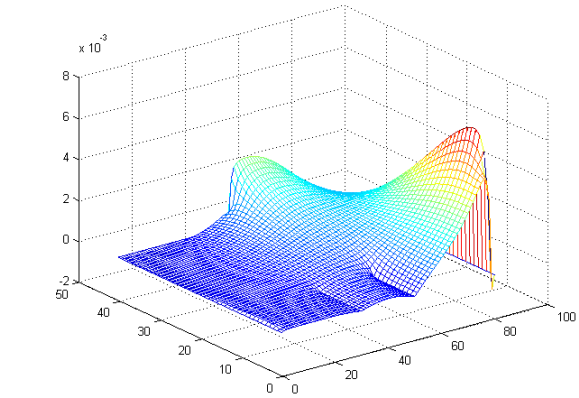

Figure 13: Difference in the imaginary part of the potential distribution between FEM and IFEM (L=5) for the second model (conductivity ratio 1:0.1).

ISSN: 1727-1983

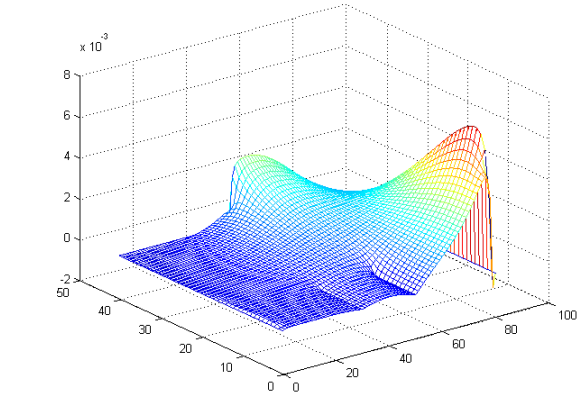

Figure 14: Difference in the imaginary part of the potential distribution between FEM and IFEM (L=5) for the second model (permittivity ratio 1:0.1).

The results obtained for the third model depend on the contrast between the dielectric parameters of the different regions of the model and the number of layers used for modelling its surroundings. The greatest differences in potential distribution between the FEM and the IFEM were obtained at the boundaries simulating the surroundings. An example of such a difference in potential distribution is presented in Figure 15. The potential distribution between the electrodes in the central region was the same. We observed the influence of the L parameter on the results obtained. If only the conductivity or permittivity of the surround was changed, then there was also a difference between the phases of potential outside the region marked "1" for the FEM and the IFEM. These results were consistent with those obtained for the first and second models.

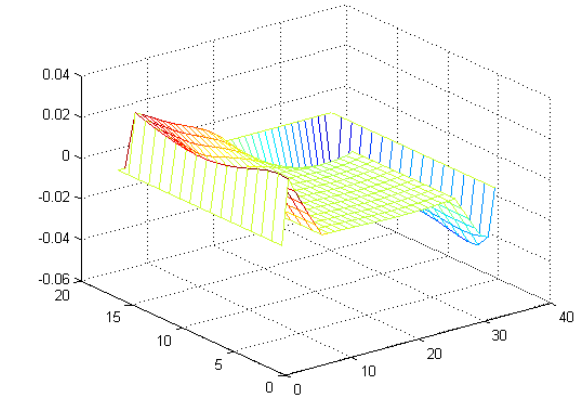

Figure 15: Example of differences in potential distribution for FEM and IFEM, third model.

The difference in potential distribution between coarse and dense mesh is shown in Figures 16 and 17. The greatest difference is in the surrounding area in both cases. It can be seen that results obtained for the FEM and IFEM models differ. This indicates that the mesh should have the correct density, although the general results of the comparison of FEM and IFEM are followed for coarse and dense meshes.

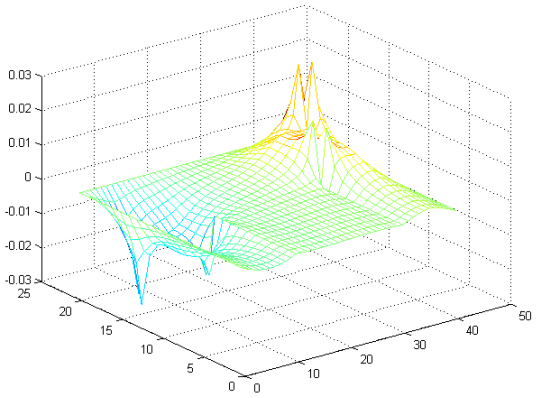

Figure 16: Example of differences in potential distribution for the FEM for different mesh density, third model.

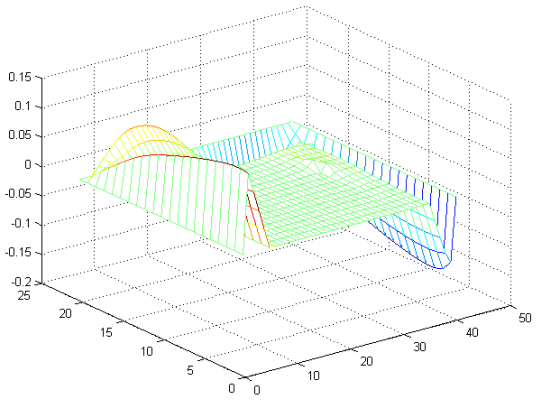

Figure 17: Example of differences in potential distribution for the IFEM for different mesh density, third model.

For the fourth model (the measurement cell), no differences were observed in current density distribution inside the measurement cell for any of the methods or any of the values of L considered. The difference appears in the construction material and surround. (Figs. 18 and 19). It can be seen that the first method gives slightly different results from the second and third methods. This may lead to additional error when the correction method based on numerical simulation is applied to real measurement. It results from an incorrect estimate of the ratio of the current flowing through the material for measurement and the surround (including the cell construction material). Figure 20 presents the results for the different sizes of the third version of the cell model.

ISSN: 1727-1983

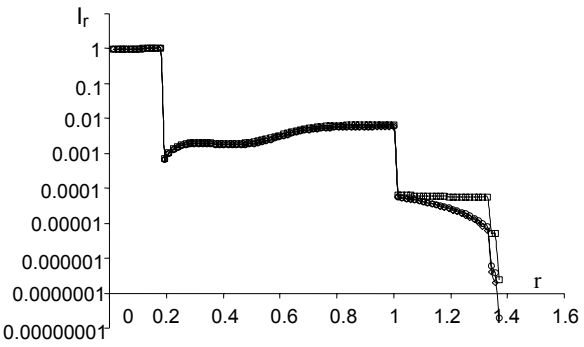

Figure 18: Normalised real part of current density as a function of normalised distance from the centre of the probe for 1 kHz; first method – squares, second method – circles, third method – diamonds.

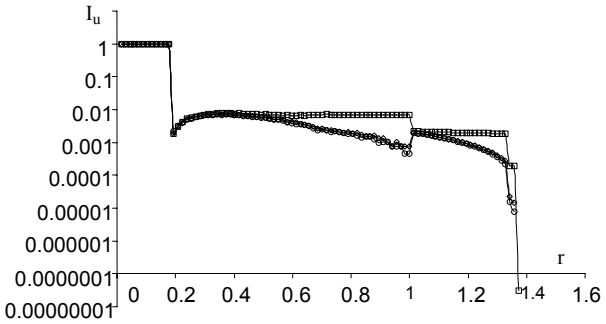

Figure 19: Normalised imaginary part of current density as a function of normalised distance from the centre of the probe for 1 kHz; first method – squares, second method – circles, third method – diamonds.

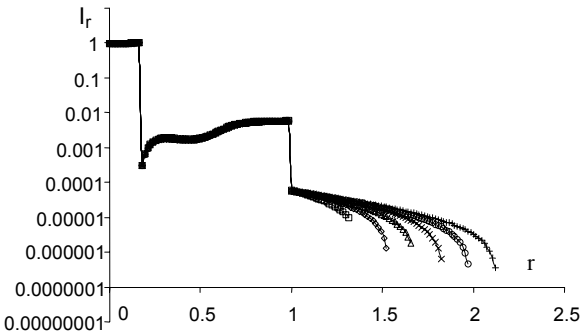

Figure 20: Normalised real part of current density as a function of normalised distance from the centre of the probe for 10 kHz, third method.

Conclusions

The surroundings have to be taken into account where there is a low degree of contrast between its parameters and those of the object modelled. In traditional FEM the modelling of the surroundings requires a larger number of elements than in IFEM. Thus the memory requirement and time of computation is also greater. In extreme cases the number of elements simulating the surroundings can be ten times greater than those used for simulating the object under examination. The IFEM approach allows the number of elements to be reduced, although it should be remembered that different types of elements in IFEM may lead to different results, and also that the choice of parameter L in the exponential decay function should be made carefully, since there is a non-linear dependence on it. Another practical problem may also appear, arising from the overflow error during the calculation for small values of L.

References

[1] BETTES, P. (1992): 'Infinite Elements', Penshaw Press, Sunderland, UK

[2] BETTES, P. (1977): 'Infinite Elements', *International Journal for Numerical Methods in Engineering*, **11**, pp. 53-64.

[3] VAUHKONEN J. P., VAUHKONEN M., and KAIPIO J. (2000): 'Errors due to the truncation of the computational domain in static three-dimensional electrical impedance tomography', *Physiol. Meas.*, **21**, pp. 125-135

[4] POLIŃSKI A. WTOREK J. KOCHAŃSKA B. PENKOWSKI M., and TRUYEN B. (2004): 'Measurement cell – current density analysis' Proc. of XII International Conference on Electrical Bio-Impedance, Poland, 2004, pp. 309-312

ISSN: 1727-1983